

PSCAD Simulation of Grid-Tied Photovoltaic Systems and Total Harmonic Distortion Analysis

Abdulrahman Y. Kalbat, *Member, IEEE*

Abstract--With the increasing fears of the impacts of the high penetration rates of Photovoltaic (PV) systems, a technical study about their effects on the power quality metrics of the utility grid is required. Since such study requires a complete modeling of the PV system in an electromagnetic transient software environment, PSCAD was chosen. This paper investigates a grid-tied PV system that is prepared in PSCAD. The model consists of PV array, DC link capacitor, DC-DC buck converter, three phase six-pulse inverter, AC inductive filter, transformer and a utility grid equivalent model. The paper starts with choosing PSCAD as the simulation environment and then by investigating the tasks of the different blocks of the grid-tied PV system model. It also investigates the effect of variable atmospheric conditions (irradiation and temperature) on the performance of the different components in the model. DC-DC converter and inverter in this model use PWM and SPWM switching techniques, respectively. Finally, total harmonic distortion analysis on the inverter output current at PCC was applied and the values obtained were compared with the limits specified by the regulating standards such as IEEE Std 519-1992

Index Terms--EMTDC, photovoltaic systems, power system harmonics, power system simulation, PSCAD, smart grids, total harmonic distortion.

I. SELECTION OF SIMULATION ENVIRONMENT

Several power system simulation packages are available in the market which vary in their capabilities, simulation speeds, prices and how rich their libraries are. Some examples of widely used simulation platforms are Simulink SimPowerSystems, PSCAD and RSCAD. These packages were compared in [1] using a simple two area system which consists of four machines connected by a transmission line. Despite its small size, this system was specifically designed to mimic very closely the behavior of typical systems in actual operation.

RSCAD has the capability of simulating the behavior of power systems and control in real time and allows interface with hardware for closed loop studies. PSCAD is a powerful and flexible graphical user interface to the world-renowned EMTDC simulation engine but it does not provide power flow solutions. On the other hand, Simulink SimPowerSystems provides power flow solutions but the simulation gets slower as the system size gets larger. Both Simulink SimPowerSystems and PSCAD don't allow interface to hardware for closed loop studies.

By simulating the previous simple network for 10 seconds in all platforms and on the same PC, it was found by the study that the time require to complete the simulation for RSCAD, PSCAD and Simulink SimPowerSystems was 10, 35 and 37 seconds, respectively.

Based on the previous study, RSCAD is the fastest and the most efficient way of simulating power systems if the cost of the simulator can be overcome. Because of the slow simulation time achieved by Simulink SimPowerSystems, PSCAD was chosen to simulate the Grid-Tied PV system in this paper. Another advantage of PSCAD is its ability to interface with Simulink. This feature enables the researchers to combine the flexible power systems simulation of PSCAD with the rich and ready-to-use control systems library of Simulink which helps in minimizing the modeling time. Also, PSCAD's interface is designed in a way that is easily used by the researchers and the developers in power systems.

II. PSCAD MODEL OF GRID TIED PHOTOVOLTAIC SYSTEM

The PSCAD model used in this paper is based on [2] and it mainly consists of PV array model, DC link capacitor, DC-DC converter, three phase inverter, AC filter, transformer and utility grid equivalent model, as shown in Fig. 1. In this section, the tasks and some of the important parameters which

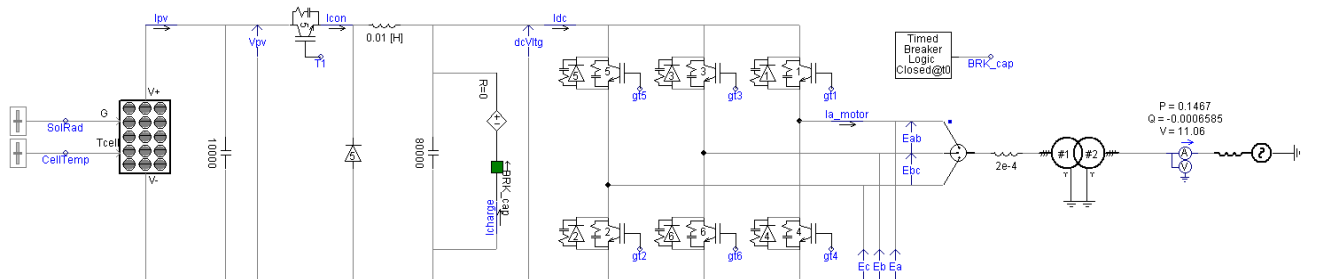


Fig. 1. Grid-Tied PV model in PSCAD

define each component's model will be discussed. The tasks of the different additional circuits which are used to control some components in the main model will be also discussed. The effects of variable atmospheric operation conditions (irradiation and temperature) will be discussed for some components.

A. PV Array

Photovoltaic cell is the basic semiconductor device that generates electricity by the photovoltaic effect when exposed to radiant energy such as sunlight [3]. The default parameters which were used to define the PV module in PSCAD are shown in Table I. The model enables the user to specify the number of series and parallel cells per module and the number of modules connected in series and in parallel which helps in building PV systems with high power rating. By using the default values, the final output of the single module is 650 watt and 260 kilo-watt for the total 400 modules.

The effect of varying the input irradiation and temperature on the short circuit current and open circuit voltage, respectively, is shown in Fig. 2 and Fig.3. Increasing the irradiation increased the short circuit current while increasing the temperature decreased the open circuit voltage. Next, is a detailed discussion about the expected range of some of the parameters shown in Table I. Please notice that some of the values in the table might be out of the expected range due to the fact that the default values were calculated for a single or group of PV modules combined together and then input in the model as the value for a single solar cell. This is done to be able to build PV systems with high power ratings since the maximum number of modules in series and in parallel in the PSCAD PV model are 20.

TABLE I
Parameters of the PV Module in PSCAD Model

PV array parameters	PV array name (optional)	PVarray1
	No. of modules connected in series / array	20
	No. of module strings in parallel / array	20
	No. of cells connected in series / module	108
	No. of cell strings in parallel / module	4
	Reference irradiation (W/m^2)	1000
	Reference cell temperature ($^{\circ}\text{C}$)	25
PV cell parameters	Effective area / cell (m^2)	0.01
	Series resistance / cell (Ω)	0.02
	Shunt resistance / cell (Ω)	1000
	Diode ideality factor	1.5
	Band gap energy (eV)	1.103
	Saturation current at reference conditions / cell (A)	1e^{-9}
	Short circuit current at reference conditions / cell (A)	2.5
	Temperature coefficient of photo current (A/K)	0.001
	Temperature coefficient of open circuit voltage (V/K)	-0.003
Monitoring	Photo current / module (A)	-
	Internal diode current / module (A)	-
	Internal diode voltage / module (V)	-
	Internal power loss / module (W)	-
	Output power / module (W)	-
	PV array output current (A)	Iarray
	PV array output voltage (V)	Varray

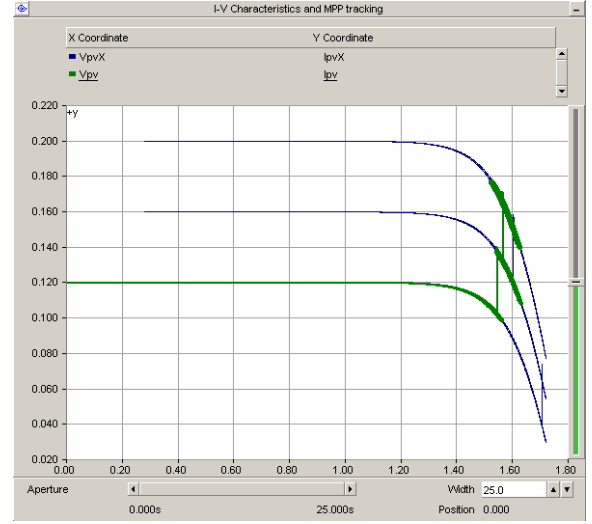


Fig. 2. IV characteristics of the PV at different irradiancies and at 25°C . Increasing the irradiation from 600 W/m^2 to 800 W/m^2 and then to 1000 W/m^2 increased the operation point and the short circuit current (y-axis).

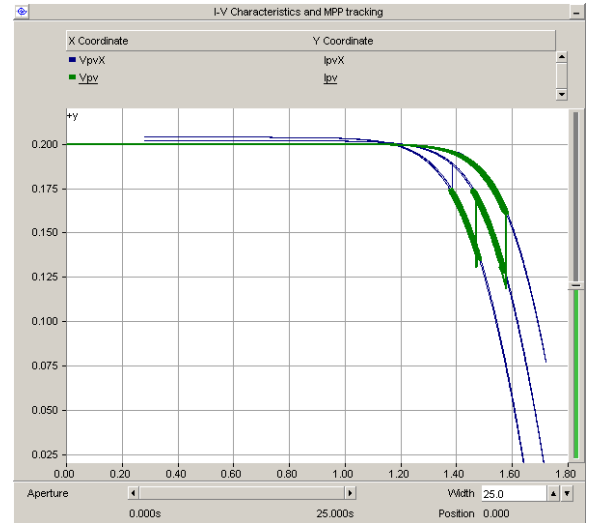


Fig. 3. IV characteristics of the PV at different temperatures and at 1000 W/m^2 . Increasing the temperature from 25°C to 50°C and then to 75°C decreased the operation point and the open circuit voltage (x-axis).

In the following text, the parameters shown in Table I will be discussed. The total number of cells/models connected in series determines the total voltage of the module/array, respectively. The total number of cells/models connected in parallel determines the total current of the module/array, respectively.

Standard Test Conditions (STC) are conditions under which a module is typically tested in a laboratory under an irradiance intensity of 1000 W/m^2 , AM1.5 solar reference spectrum and cell/module temperature of $25 \pm 2^{\circ}\text{C}$ [4]

The ideality factor of a diode is a measure of how closely the diode follows the ideal diode equation and it ranges from 1 to 2 for most solar cell structures, where it is 1 for the ideal diode and 2 for the non-ideal diode. Multi-junction cells, which are with multiple p-n junctions layered on top of one another, have ideality factors greater than 2. As the ideality factor increases, a longer bend in the knee point of the I-V curve occurs and the maximum power point decreases [5].

Based on [6], which lists up to 22 different methods for the determination of the solar cell ideality factor, the measured values depended on the kinds of solar cells investigated and the operation conditions (fixed or variable temperature, variable voltage range and dark and/or light conditions). In case of crystalline silicon (c-Si), the ideality factor ranged from 1.26 to 1.5 for a temperature and irradiation intervals of [295 to 328] K and [0 to 1000] W/m², respectively.

The I-V curve of ideal solar cell is square (Fill Factor = 1) where the maximum power point occurs at short circuit current and open circuit voltage yielding a cell conversion efficiency of 100%. But in reality, the cell I-V curve exhibits an exponential behavior (Fill Factor = 0.89) due to losses that arise from the parasitic series and shunt resistances. Series resistance is the sum of all resistance due to all the components that come in the path of current like base, emitter, semiconductor-metal contact resistance and resistance of metal contact. It is desirable to have the series resistance as low as possible, in the order of few m-ohms per cm² (from 0 to 1600 mΩ.cm²)[7]. If the series resistance increases, the maximum power point decreases and for very large values of series resistance the short circuit current starts decreasing without affecting the open circuit voltage. Shunt resistance is due to the leakage in the p-n junction because of the crystal defects and the impurities in the junction region. It is desirable to have the shunt resistance as high as possible, in the range of several hundred ohms. If the shunt resistance decreases, the maximum power point decreases and for very small values of shunt resistance the open circuit voltage starts decreasing without affecting the short circuit current [8].

Band gap energy of the solar cell is the minimum energy necessary to elevate an electron to the excited state, or upper energy level, so that it can be conducted through the solar cell to the load. Too large a band gap and the solar cell will only absorb short wavelengths of light (photon with high energy) and so a small photocurrent will be produced. Too small a band gap and the solar cell will produce a large photocurrent, but a small voltage and lower efficiencies will result [9]. Some values of this energy are 1.12 eV for Crystalline Silicon (c-Si), 1.45 eV for Cadmium Telluride (CdTe) and 1.42 eV for Gallium Arsenide (GaAs) [10].

B. DC Link Capacitor

The DC link minimizes the ripple of the PV source current by using a large capacitor. It is assumed in determining the size of DC link capacitor that the output current is ripple free. The voltage across the Dc link capacitor is controlled by the DC-DC converter as discussed next.

C. DC-DC Converter for MPP Tracking

DC-DC converter is used for Maximum Power Point Tracking (MPPT) by controlling the voltage across the DC link capacitor and the PV array. This is achieved by first creating a reference voltage that is then supplied to a PI controller which creates switching signals that force the voltage across the PV array to follow the reference voltage.

These two stages are discussed next.

1) Maximum Power Point Tracking (MPPT)

The model used for creating the reference voltage is shown in Fig. 4. First, photovoltaic output current (I_{pv}) and output voltage (V_{pv}) are passed through a first order low pass filter with a magnitude of $G = 1$ and a time constant of $T = 0.01$ seconds in order to filter out the high frequency components or harmonics from these signals as shown in Fig. 5 and Fig. 6. The filtered current and voltage signals (I_{pv_F} and V_{pv_F}) are then fed into the MPPT control block that uses the **Incremental Conductance Tracking Algorithm**. An algorithm that is based on the fact the slope of the PV array power curve shown in Fig. 7 is zero at the Maximum Power Point (MPP), positive on the left of the MPP, and negative on the right. The MPP can thus be tracked by comparing the instantaneous conductance (I/V) to the incremental conductance ($\Delta I/\Delta V$) [11] as in (1):

$$\begin{cases} \Delta I / \Delta V = -I / V, & \text{at MPP} \\ \Delta I / \Delta V > -I / V, & \text{left of MPP} \\ \Delta I / \Delta V < -I / V, & \text{right of MPP} \end{cases} \quad (1)$$

Based on the previous three cases, the MPPT generates a reference voltage (V_{mpt}) at which the PV array is forced to operate. The algorithm decrements or increments V_{mpt} to track the maximum power point when operating under varying atmospheric conditions. This reference voltage V_{mpt} is used as an input to the DC-DC Converter Control model discussed next.

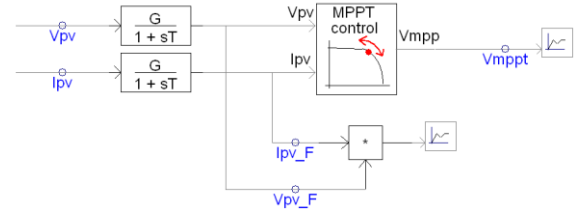


Fig. 4. Maximum power point tracking model in PSCAD

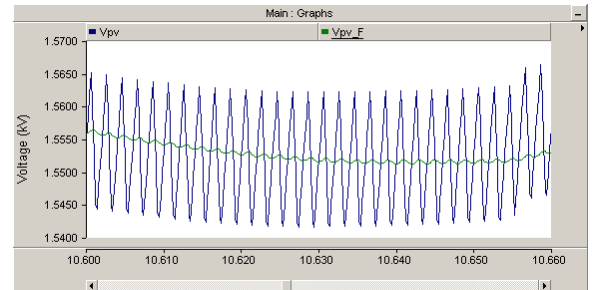


Fig. 5. Input (V_{pv}) and filtered output voltage (V_{pv_F}) of the low pass filter at STC.

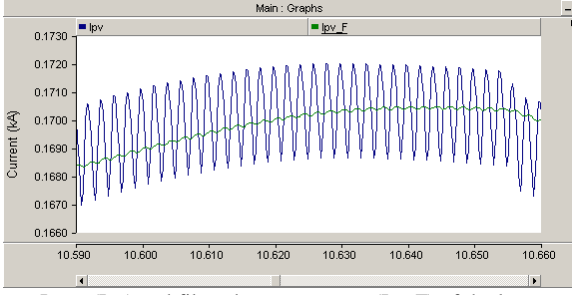


Fig. 6. Input (I_{pv}) and filtered output current ($I_{pv F}$) of the low pass filter at STC.

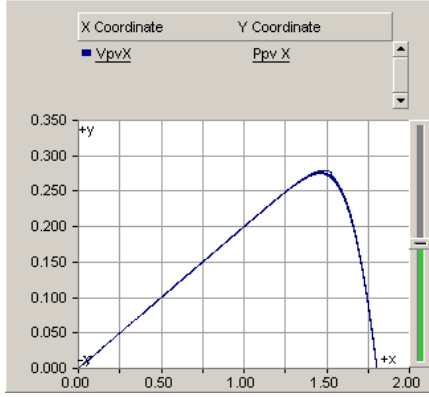


Fig. 7. Characteristic PV array power curve at STC. PV array power output in kW (y-axis) and PV array voltage in kV (x-axis).

2) DC-DC Converter Control

DC-DC converter is an electronic circuit that is used either to step down the input voltage (buck converter) or to step up the input voltage (boost converter). In this PSCAD model, buck converter was used that consists of a Pulse Width Modulation circuit (shown in Fig. 8), Insulated Gate Bipolar Transistor (IGBT) switch, inductor, capacitor and free-wheel diode [12], as shown in Fig. 1.

The difference between the solar panel output voltage (V_{pv}) and the reference voltage (V_{mppt}) is used as an input to the Proportional-Integral (PI) controller, shown in Fig. 8, which then, based on this difference, controls the duty cycle of the PWM pulse. The duty cycle, defined as the fraction of the period during which the switch is on, ranges between 0 and 1. A duty cycle value of 0.5 means on and off time are equal, a value greater than 0.5 means on time is greater and a value less than 0.5 means off time is greater [13]. The PWM signal ($T1$) was generated by using a comparator which has the duty cycle signal at port A and a saw-tooth wave at port B which ranges from 0 to 1. The comparator sets its output to 1 whenever A is greater than B and 0 otherwise creating pulses with a magnitude of 1 and with pulse widths which depend on the duty cycle.

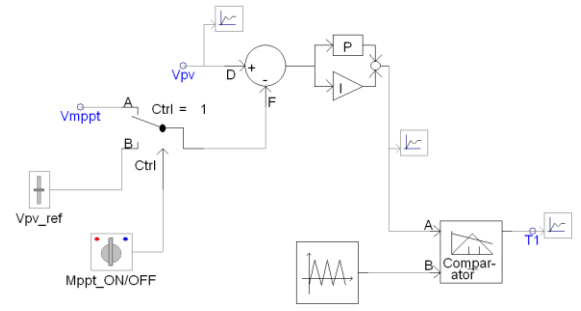


Fig. 8. DC-DC Converter Control model in PSCAD.

By supplying the gate terminal of the IGBT switch with the PWM signal ($T1$), the converter could be switched on (when $T1 = 1$) and off (when $T1 = 0$) and for the time durations which are determined by the widths of the pulses.

When the IGBT switch is on, the free-wheel diode is reverse biased (open circuit) and current flows through the inductor causing it to be charged with energy which helps in limiting the slew rate, maximum rate of change of the output voltage, of the switch. The capacitor is also charged and provides a filtering action by minimizing the voltage ripple produced at the output of the buck converter.

When the IGBT switch is off, the free-wheel diode is forward biased (short circuit for ideal diode) providing a path for the discharge current from the inductor. The capacitor is also discharged.

This continuous charging and discharging process of the inductor and the capacitor forces PV output voltage (V_{pv}) to track and follow the reference voltage (V_{mppt}) to operate at the MPP, as shown in Fig. 9, even when the irradiation decreased from 1000 W/m² to 500 W/m².

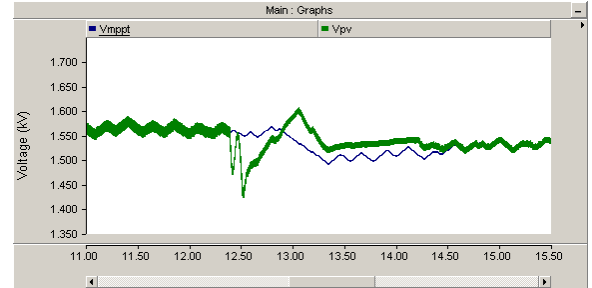


Fig. 9. MPPT reference voltage (V_{mppt}) and PV array output voltage (V_{pv}) at 1000 W/m² and 500 W/m².

D. Three Phase Inverter

In order to be able to tie a PV system with the utility grid, the DC output power of the DC-DC converter should be converted into a three phase AC power using a three phase inverter. IT is part of inverters' task to keep the DC voltage across its input (DC-DC converter's output) at a constant value. In this PSCAD model, the three phase inverter consists of a simple P and Q regulation circuit, a firing pulse generator and a three phase inverter bridge.

1) Simple P and Q Regulation

In order to establish a constant DC bus voltage ($dcVltg$) between the DC-DC converter and the inverter, a PI controller,

shown in Fig. 10, is used to set this voltage at 0.5 kV. The output of the controller (Ang) will be used as an input to the firing pulse generator which will be discussed next.

The second PI controller sets the reactive power (Q) of the grid to zero which forces the inverter to operate at unity power factor so that it produces sinusoidal voltage and current which are in phase. The output of this controller (Mag) will be also used as an input to the firing pulse generator.

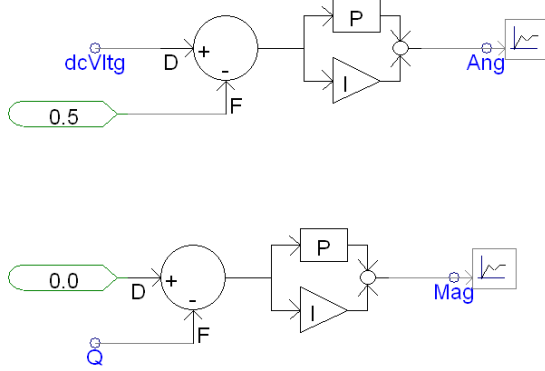


Fig. 10. Simple P and Q regulation model in PSCAD

2) Firing Pulse Generation

The switching signals of the 6 IGBT switches of the 3-legged inverter bridge shown in Fig. 1 were generated using a Sinusoidal Pulse Width Modulation (SPWM) technique shown in Fig. 11. It starts with creating three sinusoidal modulating waves with a frequency of 60 Hz and a phase shift equal to the output of the previous PI controller (Ang) with additional shifting of -120 and 120 degrees. The magnitude of the modulating waves is equal to (Mag) from the previous PI controller. Then, the three sinusoidal modulating waves were compared with a triangular carrier wave with magnitude ranging between -1 and 1. Switching signals gt1, gt3 and gt5 were generated by setting the output of the comparator to 1 whenever the modulating wave is greater than the carrier wave and 0 otherwise. Since the operation of the two switches in each of the three legs of the inverter bridge should be complementary to produce the final sinusoidal wave, the switching signals gt4, gt6 and gt2 were generated by inverting the switching signals gt1, gt3 and gt5, respectively [14].

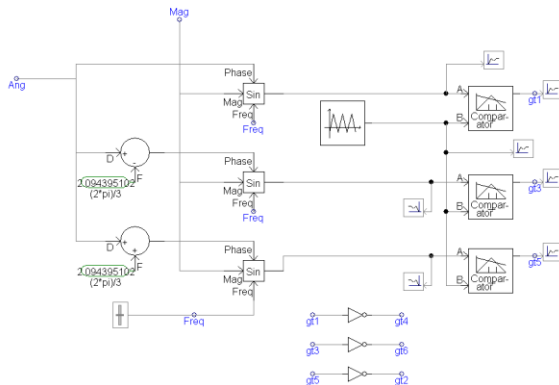


Fig. 11. Firing pulse generation model in PSCAD

3) Three Phase Inverter Bridge

By applying the previously generated switching signals (gt1 to gt6) to the 6 IGBT switches shown in Fig. 1, the inverter kept its input DC voltage (dcVltg) at a constant value of 0.5 kV, as shown in Fig. 12, even when the irradiation increased from 200 W/m² to 1000 W/m². It also converted the constant DC voltage at its input (dcVltg) to an AC voltage as shown in Fig. 13. It should be noticed from Fig. 13(a) that the produced AC voltage is not a perfect sinusoidal and from Fig. 13(b) it is clear how the voltage decreased and how the signals were distorted around second 10.2 when the irradiation was decreased from 1000 W/m² to 500 W/m².

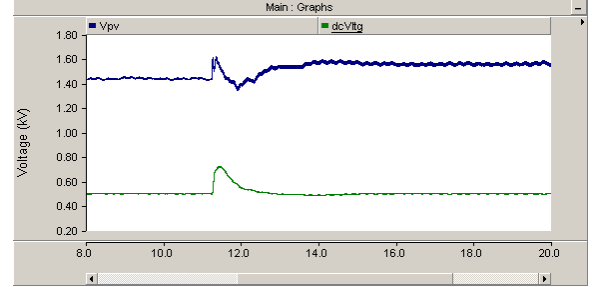
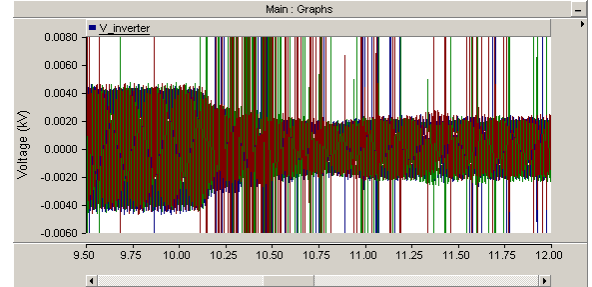
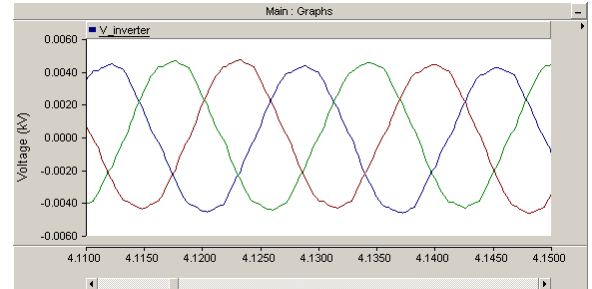


Fig. 12. PV array output voltage (Vpv) and DC-DC converter output voltage (dcVltg) at 200 W/m² and 1000 W/m².



(a)



(b)

Fig. 13. Inverter output Line-Neutral voltage (a) General view of the inverter output Line-Neutral voltage at 1000 W/m² and 500 W/m² (b) Close up view of the inverter output Line-Neutral voltage at 1000 W/m².

E. AC Filter

Based on the previous observations related to the output voltage of the inverter and the distortion involved, an AC filtering stage is required to further smoothen the output and limit the voltage drop in the AC side of the inverter when operating under variable atmospheric conditions [15]. In this paper, the AC filter is implemented using the inductor shown in Fig. 1. Although the irradiation was decreased from 1000 W/m² to 500 W/m² around second 10, the inductor resisted the

drop in the voltage and maintained it constant as shown in Fig. 14(a). The inductor also improved the shape of the output voltage to an almost sinusoidal wave as shown in Fig. 14 (b). By comparing Fig. 14 (a) to Fig. 13 (a), one should notice how the harmonic distortion was greatly removed from the output voltage especially at the time when the irradiation was changed.

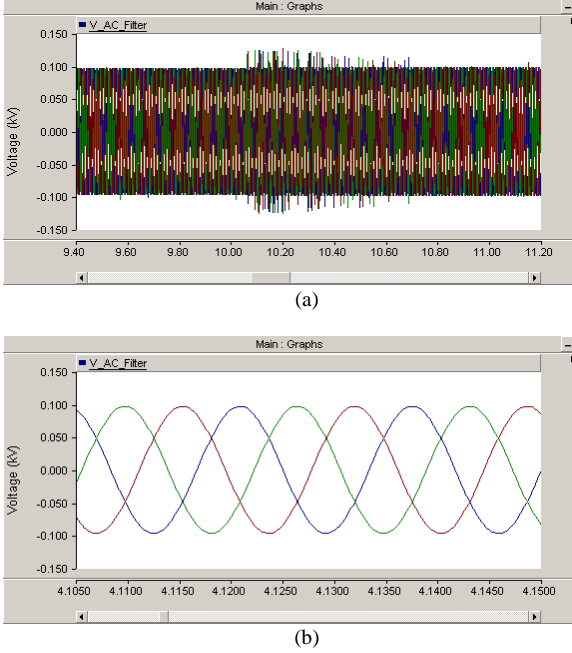


Fig. 14. AC filter output Line-Neutral voltage (a) General view of the AC filter output Line-Neutral voltage at 1000 W/m² and 500 W/m² (b) Close up view of the AC filter output Line-Neutral voltage at 1000 W/m².

F. Transformer

Transformers in grid connected PV systems act as galvanic isolation and can be used for voltage adjustment if required. There are three main methods used by the inverters for galvanic isolation: low frequency transformer, high frequency transformer and transformer-less inverters. Most commonly used method for galvanic isolation is using the conventional low frequency transformer operating on grid frequency. By controlling AC current, the power that is fed into the grid can be controlled. This is a tried and tested method and is being used right from the start of the PV technology. But this has some disadvantages like high weight, high cost, additional losses and non-unity power factor, especially at low load conditions. One way to omit the bulky transformer is to use high frequency transformers. Another emerging topology is the transformer-less inverter which has less overall losses, lighter in weight and it is cheaper than conventional grid frequency transformer topology. In addition, topology without transformer increases the control over the system voltage and power since transformer limits the control of the grid current [16][17].

A conventional, operating on grid frequency (60 Hz), step up, wye-wye, three phase transformer (230 V / 11 kV) was used in the PSCAD model as shown in Fig. 1. The low voltage

side of the transformer (230 V) was connected to the inverter while the high voltage side (11 kV) was connected to the grid.

G. Utility Grid

The utility grid system is represented only as an equivalent 11 kV and 60 Hz source behind the system inductive impedance as shown in Fig.1. Based on [18], which provides ranges of voltage ratings for electric power systems in the US as shown in Table II, the utility grid (11 kV) in this PSCAD model falls within the medium voltage (MV) power systems range.

TABLE II
Voltage Rating for Electric Power System and Equipment

Voltage Class	Nominal Line-Line RMS Voltage
Low Voltage	< 600 V
Medium Voltage	600 V – 69 kV
High Voltage	69 kV – 230 kV
Extra High Voltage	230 kV – 1100 kV
Ultra High Voltage	> 1100 kV

III. TOTAL HARMONIC DISTORTION (THD) ANALYSIS

Harmonics are sinusoidal components of a periodic wave having a frequency that is a multiple of the fundamental frequency. Harmonics in PV systems are generated by the converters which use switching techniques that generate signals that are not perfect sinusoids. Connecting PV systems to the utility grid, which is already being injected with harmonics by the non-linear loads connected to the power network, will add a stress on the power quality of the grid.

In order to maintain acceptable levels of grid power quality, standards that regulate the effects of PV systems on the utility grid should be developed. One such standard is IEEE Std 929-2000 “IEEE Recommended Practice for Utility Interface of Photovoltaic (PV) Systems” [19] which ensures compatible operation of photovoltaic (PV) systems that are connected in parallel with the electric utility. It is recommended by the previous standard that the harmonic distortion at the Point of Common Coupling (PCC), which is the point at which the PV system is tied with the grid, should comply with IEEE Std 519-1992 [20]. In this PSCAD model, PCC lies between the transformer and the grid.

The PV system output should have low current distortion levels to ensure that no adverse effects are caused to other equipment connected to the utility system. The key requirements of clause 10 of IEEE Std 519-1992 are summarized as the following:

- Total harmonic current distortion shall be less than 5% of the fundamental frequency current at rated inverter output.
- Each individual harmonic shall be limited to the percentages listed in Table III. The limits in Table III are a percentage of the fundamental frequency current at full system output. Even harmonics in these ranges shall be <25 % of the odd harmonic limits listed.

TABLE III
Current Distortion Limits at PCC for six-pulse converters

as recommended in IEEE Std 519-1992

Odd Harmonics	Distortion Limit
3 rd – 9 th	< 4.0 %
11 th – 15 th	< 2.0 %
17 th – 21 st	< 1.5 %
23 rd – 33 rd	< 0.6 %
Above the 33 rd	< 0.3 %

In order to calculate the Total Harmonic Distortion (THD) of the current at the PCC, the PSCAD standard blocks shown in Fig. 15 were used. The Fast Fourier Transform (FFT) block was used to determine the harmonic magnitude of the line current at PCC in each phase (a, b and c) as a function of time. The resulting harmonic magnitude was then used as an input to the Harmonic Distortion block which measures both the total and individual harmonic distortion in percentage (%).

The FFT block was configured to output the magnitude of 15 harmonics with the fundamental frequency at 60 Hz. Inputs to this block were the three RMS values of the three line currents at PCC. Harmonic Distortion block was configured to output THD and individual harmonic distortions in percent.

In Fig. 16 is shown the THD of the current in phase a at PCC and measured at STC which was plotted as a percentage that varies with time. It is noticed from this figure that the THD is oscillating around 4% which is less than the 5% limit established by the previously discussed standard.

In Fig. 17 is shown the harmonic distortion of the current in phase a at PCC and measured at STC which is visualized using a polymeter in PSCAD that associates the harmonic distortion (%) with its harmonic index (1 to 15). By comparing the value of each harmonic in Fig. 17 with the range given in Table III, it was found that none of the harmonics violates the specified limits.

By expanding the harmonic index to 63 as shown in Fig. 18, it was found that harmonics with indices from 38 to 46 were violating the distortion limits, which is 0.3%. Based on this, one can conclude that these distortions were introduced to the PCC because of the insufficient filtering stages implemented in the PSCAD model. Another reason is the simplicity of the controls used in generating the switching signals of the inverter.

One way of improving the quality of the inverter output current is by using the range of the indices of violating harmonics previously found (38 to 46) to design a band stop or a low pass filter that is capable of removing the harmonics in that range of frequencies.

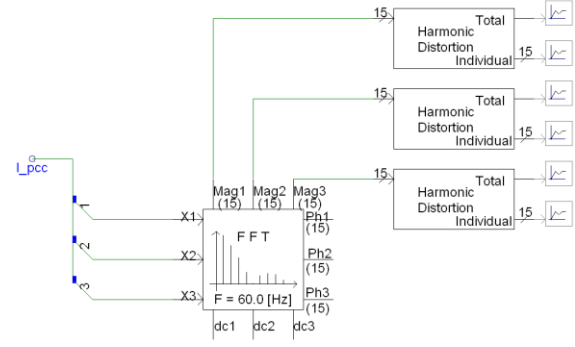


Fig. 15. PSCAD circuit to calculate total current harmonic distortion at PCC

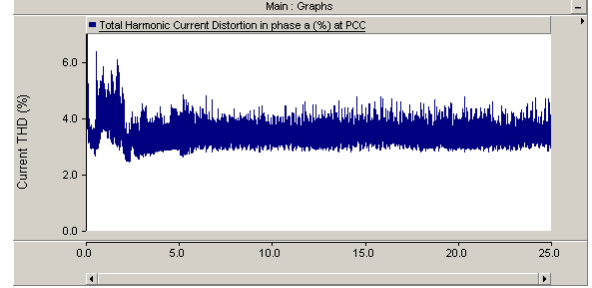


Fig. 16. THD (%) of the current in phase a at PCC and measured at STC.

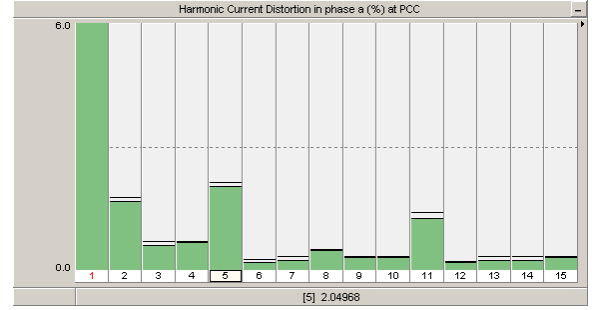


Fig. 17. Individual harmonic distortion (%) of the current in phase a at PCC and measured at STC. In the x-axis is shown the index of the harmonic with the fundamental frequency having harmonic index that is equal to 1.

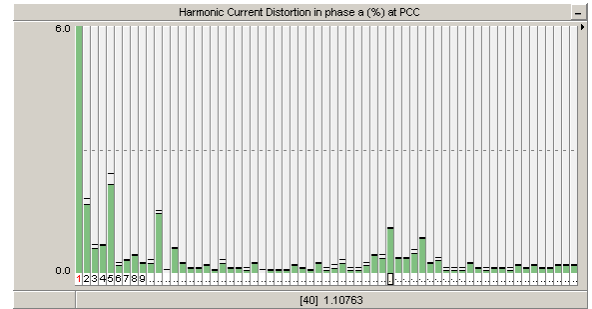


Fig. 18. Individual harmonic distortion (%) of the current in phase a at PCC and measured at STC. The number of the monitored harmonics was expanded to 63.

IV. CONCLUSION

In this paper, three different power systems simulation packages were compared and PSCAD was selected to investigate a model of grid-tied PV system. Then, tasks of the

different components of the model were discussed. Also, the effect of varying the atmospheric conditions (irradiation and temperature) on the PV system was justified with graphs. The control stages involved in generating the switching signals using PWM and SPWM for DC-DC converter and inverter, respectively, were tracked using the PSCAD model. Some of the standards which regulate the interfacing of PV systems with the utility grid were discussed. Finally, total harmonic distortion analysis on the output current of the inverter at PCC and at STC was conducted using standard PSCAD blocks (FFT and Harmonic Distortion blocks) and then compared with the limits specified by the standards.

V. REFERENCES

- [1] G. K. Venayagamoorthy, "Comparison of power system simulation studies on different platforms – RSCAD, PSCAD/EMTDC, and Simulink SimPowerSystems," in *Proc. 2005 Int. Conf. on Power Systems, Operation and Planning*, pp. 38-41
- [2] A. D. Rajapakse and D. Muthumuni, "Simulation tools for photovoltaic system grid integration studies," in *Proc. 2009 Electrical Power & Energy Conf.*, pp. 1-5.
- [3] *Standard Terminology of Solar Energy Conversion*, ASTM Standard E772, 2011.
- [4] *Crystalline silicon terrestrial photovoltaic (PV) modules - Design qualification and type approval*, IEC Standard 61215, 2005
- [5] S. M. Salih, F. F. Salih, M. L. Hasan and M. Y. Bedaiawi, "Performance Evaluation of Photovoltaic Models Based on a Solar Model Tester," *International Journal of Information Technology and Computer Science*, vol. 4, pp.1-10, 2012.
- [6] M. Bashahu and P. Nkundabakura, "Review and tests of methods for the determination of the solar cell junction ideality factors," *Solar Energy*, vol. 81, pp. 856-863, Jul. 2007.
- [7] M. Bashahu and A. Habyarimana, "Review and test of methods for determination of the solar cell series resistance," *Renewable Energy*, vol. 6, pp. 129-138, Mar. 1995.
- [8] C. S. Solanki, "Design of Solar Cells," in *Solar Photovoltaics: Fundamentals, Technologies and Applications*, 2nd ed. New Delhi: PHI, 2011, pp. 101-104.
- [9] G. P. Smestad, "Absorbing Solar Energy," in *Optoelectronics of Solar Cells*, Washington: SPIE Press, 2002, pp. 23-24.
- [10] T. Markvart, "Solar Cells," in *Solar Electricity*, 2nd ed. Chichester: Wiley, 2000, pp. 27-28.
- [11] T. Eswam and P.L. Chapman, "Comparison of Photovoltaic Array Maximum Power Point Tracking Techniques," *IEEE Trans. on Energy Conversion*, vol.22, pp. 439-449, Jun. 2007.
- [12] M. M. Elamari, "Optimisation of Photovoltaic- Powered Electrolysis for Hydrogen Production for a Remote Area in Libya," Ph.D. thesis, School of Mech., Aero. and Civil Eng., The Univ. of Manchester, Manchester, UK, 2011.
- [13] M. H. Rashid, "Power Supplies in *Power Electronics Handbook: Devices, Circuits, and Applications Handbook*, 3rd ed. Massachusetts: Elsevier, 2011, pp. 623-624.
- [14] B. Wu, "Two-Level Voltage Source Inverter," in *High-Power Converters and AC Drives*, 1st ed. New Jersey: Wiley, 2006, pp. 95-97.
- [15] S. A. Rahman and R. K. Varma, "PSCAD/EMTDC model of a 3-phase grid connected photovoltaic solar system," in *Proc. 2011 North American Power Symp.*, pp. 1-7.
- [16] D. Jose, "Comparison of a Three Phase Single Stage PV System in PSCAD and PowerFactory," Degree project, School of Elect. Eng., KTH Royal Institute of Technology, Stockholm, Sweden, 2012.
- [17] F. Schimpf, L. E. Norum, "Grid Connected Converters for Photovoltaic, State of the Art, Ideas for Improvement of Transformer-less Inverters," in *Proc. 2008 Nordic Workshop on Power and Industrial Electronics*, pp. 1-6.
- [18] *Voltage Rating for Electric Power Systems and Equipment*, ANSI Standard C84.1, 1989.
- [19] *IEEE Recommended Practice for Utility Interface of Photovoltaic (PV) Systems*, IEEE Standard 929, 2000.
- [20] *IEEE Recommended Practices and Requirements for Harmonic Control in Electrical Power Systems*, IEEE Standard 519, 1992.

VI. BIOGRAPHY



Abdulrahman Y. Kalbat received the B.S. degree in electrical engineering from the United Arab Emirates University, Al-Ain, in 2011. He is currently pursuing the M.S. degree with the Department of Electrical Engineering, Columbia University in the City of New York.

His current research interests are in power systems, smart grid and renewable energy systems.